Atomically-Flat Low-Resistive Germanide Contacts Formed By Laser Thermal Anneal

Maryam Shayesteh, Karim Huet, Inès Toqué-Tresonne, Razvan Negru, Chris L. M. Daunt, Niall Kelly, Dan O'Connell, Ran Yu, Vladimir Djara, Patrick B. Carolan, Nikolay Petkov, and Ray Duffy

***Abstract*— In this work state-of-the-art laser thermal annealing is used to form germanide contacts on n-doped Ge, and is systematically compared to results generated by conventional rapid thermal annealing. Surface topography, interface quality, crystal structure, and material stoichiometry are explored for both annealing techniques. For electrical characterization, specific contact resistivity and thermal stability are extracted. It is shown that laser thermal annealing can produce a uniform contact with a remarkably smooth substrate interface, with specific contact resistivity 2-3 orders of magnitude lower than the equivalent rapid thermal annealing case. It is shown that a specific contact resistivity of 2.84×10^{-7} Ω.cm^2 is achieved for optimized laser thermal anneal energy density conditions.**

***Index Terms*—Contact resistance, germanium, sheet resistance, Transfer Length Method (TLM), laser thermal annealing.**

I. Introduction

While it is still open to debate whether or when Ge will be part of an advanced logic device process in production, it is indeed clear that one of the stumbling blocks associated with the successful integration of Ge devices is the high contact resistance to n-type Ge layers. However, judging from the publications in the past 12 months alone, many real solutions are being explored by several research groups worldwide. More importantly rapid progress is being made as record-low specific contact resistivities are regularly reported.

High contact resistance on n-type Ge is mainly attributed to Fermi-level pinning (FLP) [1], and subsequently to a large electron Schottky barrier height (eSBH). An extensive literature review of the potential solutions and the state-of-the-art in this area was presented in our recent work [2], and rather than repeat ourselves here, we will now focus on a brief summary and the most recent developments in the field.

Manuscript received xxxx xx, 2012.This work has been funded by the Science Foundation Ireland under Research Grant No. 09/SIRG/I1623 and 09/SIRG/I1621, and enabled by the programme for Research in Third-Level Institutions.

M. Shayesteh, C. L. M. Daunt, N. Kelly, D. O'Connell, R. Yu, V. Djara, Patrick B. Carolan, N. Petkov, and R. Duffy are with Tyndall National Institute, University College Cork, Lee Maltings, Cork, Ireland. (email: maryam.shayesteh@tyndall.ie; ray.duffy@tyndall.ie) K. Huet, I. Toqué-Tresonne and R. Negru are with Excico, 14 Rue Alexandre Bat D. 92230, Gennevilliers, France.

Theoretical studies have shown that a thin insulating tunnel barrier can depin the Ge surface with optimum thicknesses of approximately 1 nm [3]. Selenium segregation was recently used to reduce electron Schottky barrier heights for NiGe/n-Ge contacts [4], while CF_4 plasma treatment of the Ge surface was experimentally demonstrated to alleviate FLP [5].

Gallacher *et al.* extracted specific contact resistivity (ρ_c) of 2.3×10^{-7} Ω.cm^2 on n-type Ge that was doped during epitaxial growth [6]. The optimum NiGe formation temperature was a 340 °C rapid thermal anneal (RTA). However the NiGe interface with the underlying substrate was not smooth. Recently Zheng at al. reported ohmic contacts to n-type Ge using Yb-germanide [7].

Laser thermal annealing (LTA) is of great interest in semiconductor processing as it enables ultrafast annealing with very limited thermal budgets [8]. It can suppress dopant diffusion and generates high levels of dopant activation. Specifically in Ge, Mazzocchi *et al*. reported high activation levels of B and P dopants (>1×10^{20} cm^{-3}) as well as limited diffusion when they used LTA with energy densities (ED) in the range of 0.57-1.8 J/cm^2 [9]. Firrincieli *et al*. reported ρ_c of 8×10^{-7} Ω.cm^2 on n-type Ge where LTA was used for dopant activation, in combination with RTA for NiGe formation [10]. In that work the NiGe layers were thermally stable up to 350 °C, but the interface with the Ge substrate was not flat. This is common for NiGe layers formed by RTA. Finally, Lim et al have demonstrated Fermi-level depinning using multi-pulsed LTA by the formation of epitaxial $NiGe_2$ [11].

Note that laser light can be reflected by metal layers [12]. For the thickness of Ni in this work (20 nm) the reflection difference is not expected to have a significant effect.

In this work we use LTA for NiGe contact formation on n-type Ge substrates, and systematically compare to results generated by conventional RTA, with respect to surface topography, interface quality, crystal structure, material stoichiometry, specific contact resistivity, and thermal stability. While the steps accompanying the growth of germanides, and closely related silicides, by RTA have been studied to some extent, the formation pathway for the LTA processed materials has not been thoroughly investigated.

II. Experimental Details

Fig. 1 summarizes the process flow undertaken in this study. After cleaning, high-resistivity (>40 Ω.cm) n-type (100) wafers received well implants to create a semi-insulating layer. The wafers then received a shallow P implant with the dose of 1×10^{15} cm^{-2} and energy of 12 keV. This was performed through a native oxide, and should amorphize

approximately to a depth of 25 nm. Dopant activation was performed using an RTA at 500 °C for 10 s in an N_2 ambient. It seems that 500 °C is an optimum annealing temperature for n-type dopants, as lower temperatures (e.g. 400 °C) result in poor sheet resistance and activation, whereas at higher temperatures (e.g. 600 °C), diffusion is a concern. Thereafter 20 nm of Ni was deposited using thermal evaporation. Many works to date have studied germanide formation with Ni thicknesses in this range. Transfer length method (TLM) patterning and mesa dry etch was then carried out to minimize leakage currents. The Ni layer was patterned by a standard lift-off technique.

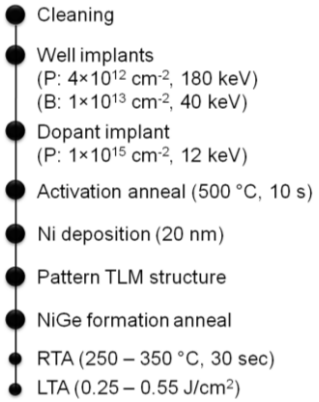

Fig. 1: A summary of the experimental process flow in this work.

The only variable in the process was the NiGe formation anneal. One set of samples received RTA treatment either at 250, 275, 300, 325 or 350 °C in N_2 for 30 s. Another set of samples received LTA processing (λ= 308 nm, single-pulse) at Excico with laser densities ranging from 0.25-0.55 J/cm^2 and time durations ranging from 144-165 ns. The laser beam area was approximately 10×10 mm^2. Note, these energy densities are significantly lower than those required for proper LTA assisted dopant activation in Ge [9]. The melting threshold was characterized by visual observation (surface color change) on test samples prior to the processing of these experimental samples

According to The Stopping and Range of Ions in Matter (SRIM), a 1×10^{15} cm^{-2} 12 keV P implant into Ge should produce a junction depth ~55-60 nm deep, even with a diffusionless anneal, so the germanide layers in this work should still be contained in the n-doped region.

Various material characterization techniques were applied to inspect surface topography and crystalline quality of the germanide layers. Top-down scanning electron microscopy (SEM) was performed on an FEI 650 FEG SEM. Atomic force microscopy (AFM) was performed in tapping/non contact mode at room temperature on 5μm×5μm scanning area. Cross-sectional transmission electron microscopy (XTEM) imaging was carried out using the JEOL 2100 high-resolution TEM under bright field conditions. Scanning TEM (STEM) imaging and Energy-dispersive X-ray spectroscopy (EDX) line scan analysis was undertaken using the Helios Nanolab system equipped with Oxford Instruments X-Max-80 EDX detector with spot size well below 1 nm. The analysis was conducted at 30 kV using moderate beam currents. For electrical characterization TLM was used to extract ρ_c. Details of the test structure description and theory can be found in our previous work [2]. For electrical characterization the KEITHLEY 37100 and KEITHLEY 2602 were used.

Furthermore, the LTA process was simulated using the enthalpy model described in [13]. This approach allows the modelling of light coupling, heat diffusion and Ge melting. It does not take into account the effects of stoichiometry change during germanide formation.

III. Results and Discussion

A. Material characterization

Firstly surface roughness and continuity of the layers was evaluated by top-down SEM and AFM. In both cases continuous layers were formed with no evidence of breakages. Fig. 2 shows representative AFM images of the surface topography which were formed by (a) RTA at 350 °C and (b) LTA at the energy of 0.35 J/cm^2. The table in Fig. 2 shows the Root mean square (RMS) data extracted for all the samples. RMS is larger for the RTA set, except for the highest ED LTA.

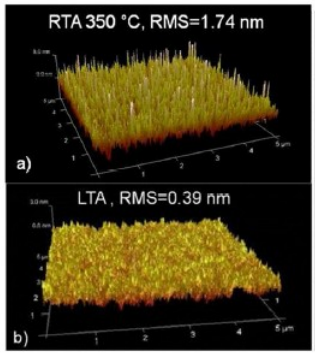

Formation Anneal	Roughness (nm)
250 °C	1.11
275 °C	1.28
300 °C	1.55
325 °C	1.47
350 °C	1.74
0.25 J/cm²	0.4
0.35 J/cm²	0.39
0.45 J/cm²	0.62
0.55 J/cm²	2.07

Fig. 2: Representative AFM images of NiGe layers formed by (a) RTA at 350 °C and (b) LTA at the energy of 0.35 J/cm^2. The table shows the surface roughness data for all the RTA and LTA samples in this work.

Much like there is a process window for NiGe formation by RTA [14, 15] where at high temperatures the thin film agglomerates into islands, this data indicates that LTA also has a process window for germanide formation above which the film degrades. 0.55 J/cm^2 is clearly too high for this application.

Fig. 3(a) shows a representative XTEM image from a germanide contact formed by a) RTA at 350 °C for 30 s in N_2, and b) LTA at 0.45 J/cm^2. The LTA process resulted in germanide formation having sharp interface with the underlying Ge substrate. In stark contrast, the germanide layer formed by RTA exhibited a rough and ridged interface with the Ge substrate with larger crystalline domains. This is nothing new, as non-smooth NiGe interfaces are commonplace when RTA is used for the formation anneal [4, 6, 16].

Additionally, the germanide layer formed by LTA showed two definite sub-layers with different stoichiometries identified by EDX line scans using a tightly focused electron probe. The quantification of the obtained EDX spectra (see Fig. 4) showed the existence of a $NiGe_2$ layer in contact with Ge covered by a NiGe surface layer. The germanide layer formed by RTA was identified as NiGe across its whole thickness.

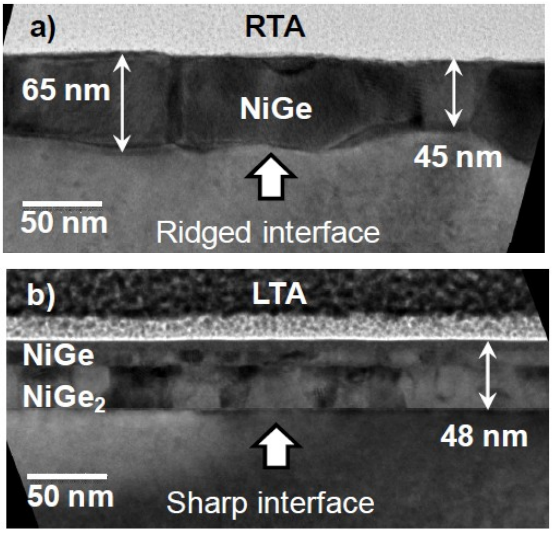

Fig. 3: Representative XTEM images of NiGe layers formed by (a) 350 °C RTA and (b) formed by 0.45 J/cm^2 LTA.

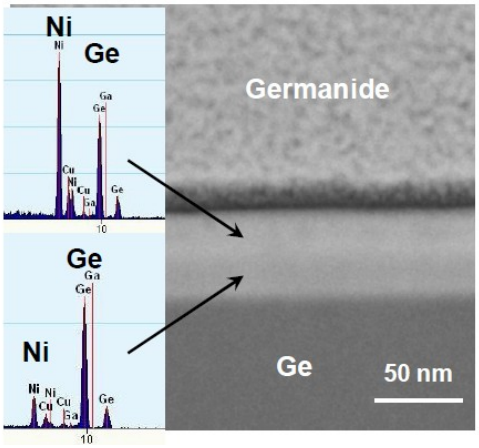

Fig. 4: EDX data and STEM of germanide layers formed by LTA at 0.45 J/cm^2, identifying $NiGe_2$ in the lower portion of the germanide layer

The germanide-substrate interface was studied at lattice resolution with the corresponding HRTEM images shown in Fig. 5. Note Figs. 5(a) and 5(b) are images from the same LTA sample, but at different locations along the interface.

Fig. 5(a) shows two grains of the $NiGe_2$ phase and the corresponding interface with the (001) oriented Ge substrate. The lattices for both $NiGe_2$ domains show some epitaxial relation. Several stacking fault defects along the (111) set of planes were observed in the Ge substrate as well as at the boundary between $NiGe_2$ domains. In comparison, Fig. 5(b) demonstrates a case where $NiGe_2$ grains have *no clear epitaxial alignment* with the underlying (001) Ge substrate despite the fact that a very sharp interface is formed. In this regard, the interface between the two layers is effectively atomically flat. Lim *et al*. [17] argued that epitaxial $NiGe_2$ on (001) Ge, although not thermodynamically favorable, may form as a result of minimization of the interfacial energy. Lattice-matched NiSi growth on Si has been reported by Gao *et al.,* where ultra-thin Ni layers were deposited on Si [18], and $NiSi_2$ preferentially formed as it has a similar lattice spacing to Si.

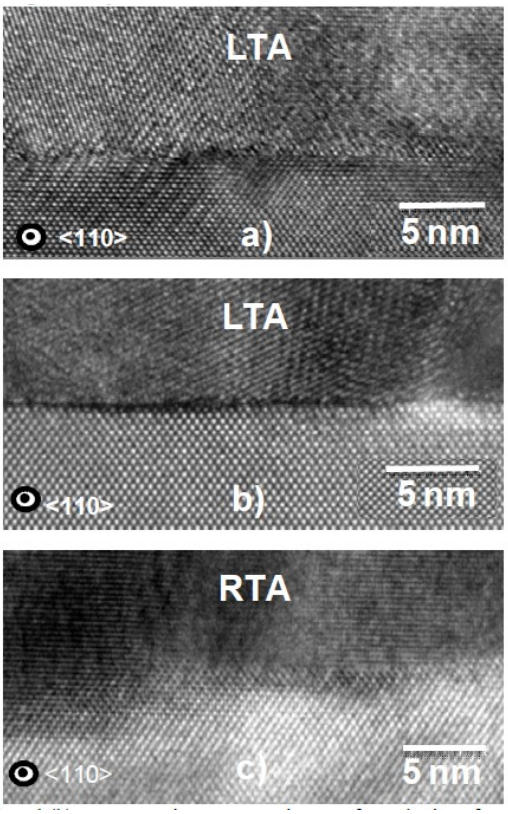

Fig. 5: (a) and (b) representative HRTEM images from the interface between Ge and the Ni-germanide after LTA 0.45 J/cm^2, and (c) RTA at 350 °C.

In contrast, the lattice resolution TEM images of the NiGe/Ge interface for the RTA treated sample revealed a corrugated surface far from being fully relaxed (Fig. 5(c)). Nevertheless epitaxial alignment of the (111) set of planes of NiGe to the (001) planes of the Ge substrate was identified. A large amount of residual strain has been observed by HRTEM lattice imaging. There is a lattice mismatch between NiGe and Ge which can be a cause of the residual strain as no Ge lattice defects are observed and the number of grain boundaries in the NiGe layer is relatively small. This is in contrast to the LTA sample where both Ge lattice defects and larger number of grain boundaries help $NiGe_2$/Ge interface to relax. Herein we outline the importance of thorough structural examination of the germanide-substrate interface properties in relation to the obtained contact resistance. Moreover the stark difference in the structure of the germanide layers obtained by LTA and RTA is a result of a fundamentally dissimilar formation pathway.

The explanation for the huge improvement in interface roughness here is linked to the thermal gradient and shallow heat distribution associated with ultra-short-pulse LTA. Using a simple enthalpy model, we could simulate the thermal dynamics during the LTA process, taking standard values for Ni and Ge optical and thermal properties. It should be noted that within this simple approach, the effect of germanide formation on thermal and optical properties is not taken into account. Most of the UV laser light is absorbed within less than 10 nm in Ge during the sub-µs timescale of the laser pulse. This surface layer acts as a heat source, which diffuses in depth over time. In Fig. 6 the maximum temperature

reached during the process is shown as a function of depth for LTA process conditions corresponding to non melt, shallow melt and deep melt regimes. The melted depth (where temperature is greater than the Ge melting temperature of 937 °C) increases with the LTA energy density. As it can be seen, the simulated thermal gradient is very high, close to 300 °C/µm, which limits the effect of the laser anneal to the near surface region. In Fig. 7, the corresponding surface temperature dynamics are reported. As is shown in the figure, the high temperature regime is sub-µs. Especially, the melting time is typically less than a few hundred ns. Within this timeframe, most of the Ni and Ge interdiffusion mechanisms are expected to take place in the *liquid* phase, during melt and recrystallization of the Ge and germanide regions.

As the melting temperature of Ni is 1455 °C, these simulations indicate that the Ni layer remains in solid form.

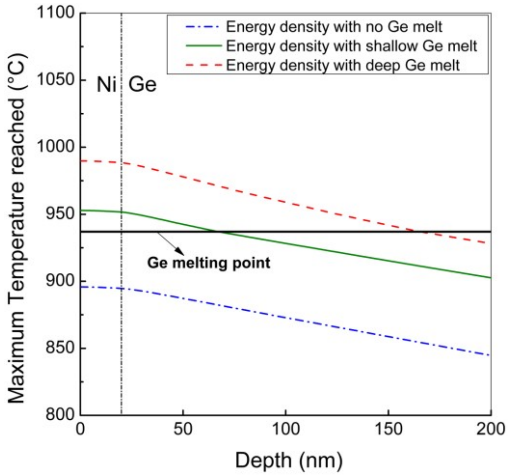

Fig. 6: Simulated maximum temperature reached as a function of depth for the applied LTA energy densities. The ED values used for simulation are 0.4, 0.45 and 0.5J/cm² for the non melt, shallow Ge melt and deep Ge melt, respectively

The ED values used for simulation are 0.4, 0.45 and 0.5 J/cm² for the non melt, shallow Ge melt and deep Ge melt, respectively. The corresponding melt depth simulated for 0.4 J/cm², 0.45 J/cm² and 0.5 J/cm² are about 0, 50 and 150 nm respectively. However, the germanide depth extracted from the TEM are much shallower in this ED range (<70nm). This discrepancy may be due to the impact of the NiGe layer optical and thermal properties which change during the process, and are not taken into account dynamically in this simple approach. Moreover, it is possible that diffusion dynamics are slower that the melting and recrystallization dynamics (sub-µs timescale), which would lead to a germanide thickness smaller than the melted depth. More advanced studies would be required to understand the germanide formation mechanisms for such an ultrafast process.

Note, in the conventional RTA case, the entire sample is essentially at the target temperature without significant thermal gradients, and the growth of germanides involves a solid-solid reaction. Much work has been devoted to understanding the effect of the liquid to solid phase transformation on impurity behaviour and solubility. Distribution coefficients have been explored since the early days of semiconductor processing, and are essentially a measure of solubility. The equilibrium distribution coefficient, k, is defined as the relative tendency of various impurities to dissolve in solid materials. In other words, k is the ratio of concentrations: C_{SOLID}/C_{LIQUID}, at the melting point of the material. In Trumbore's review paper [19], $k = C_{SOLID}/C_{LIQUID} = 3\times10^{-6}$ for Ni in Ge. Hence the solubility of Ni in Ge is vastly greater in the liquid Ge phase, compared to the solid Ge phase. Strictly speaking this value is for equilibrium conditions, but it is reasonable to state for the LTA case here. Ni is in contact with liquid Ge and thus rapidly dissolves into that layer. In effect the liquid Ge consumes the Ni on top very quickly, and the resulting Ni-germanide phase is determined by the ultra-fast reaction quenching.

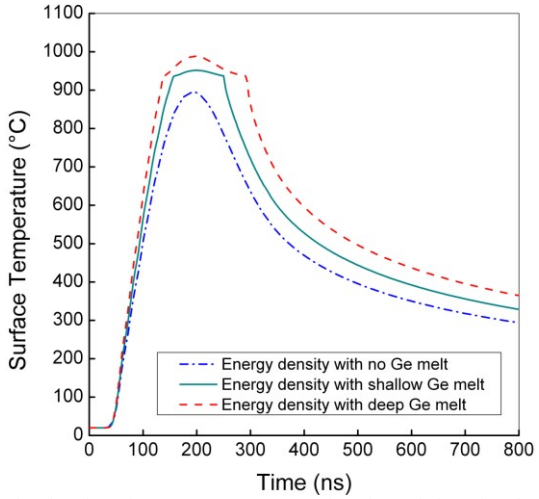

Fig. 7: Simulated surface temperature as a function of time for the applied LTA energy densities. The ED values used for simulation are 0.4, 0.45 and 0.5J/cm² for the non melt, shallow Ge melt and deep Ge melt, respectively

By changing the ED of the LTA process the surface melt depth can be controlled (Fig. 6). The result of this is having a different thickness of liquid Ge in contact with the Ni overlayer. Consequently the thickness of the obtained germanide layer scales with LTA ED as shown in Fig. 8.

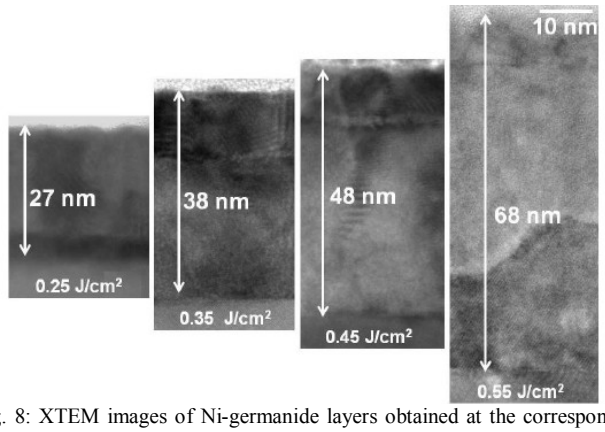

Fig. 8: XTEM images of Ni-germanide layers obtained at the corresponding laser energy densities.

B. Electrical characterization

Using the TLM test structures fabricated, ρ_c of the germanide/n-type Ge interface and the sheet resistance R_{sh} of

the underlying P doped Ge layer were then extracted. In our TLM test structure each germanide bar was 380×100 µm^2 and the spacings were 4, 16, 36, 64, 100, 144, and 196 µm. The layout consisted of a repeated array of this TLM design. Approximately 40 TLM structures within each array were electrically measured in order to extract reliable values for ρ_c and R_{sh}.

Fig. 9 shows the typical output from a TLM measurement. The inset shows current versus voltage as a function of contact spacing of a TLM structure fabricated using LTA (0.45 J/cm^2). Resistance between contacts increases with spacing.

In the main part of Fig. 9 resistance versus contact spacing is plotted for the germanide formed by RTA at 275°, 300°, 350 °C and LTA at 0.35, 0.45, and 0.55 J/cm^2. As is seen straight lines are fitted to the data. Intercepts of the line with vertical and horizontal axes are used to calculate ρ_c and R_{sh} according to theory [2].

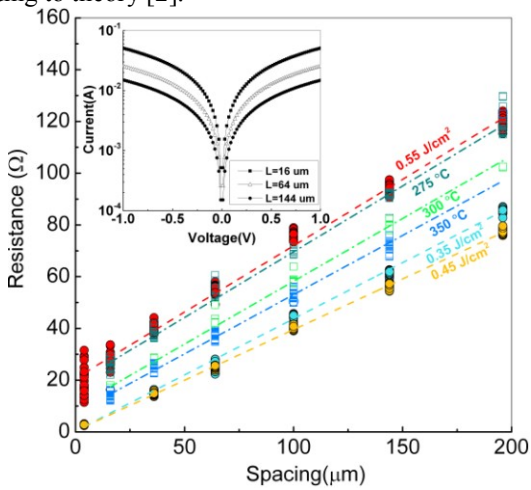

Fig. 9: Resistance versus contact spacing for LTA and RTA samples. The inset shows I-V characteristics of a typical TLM structure where the germanide contacts were formed by LTA with the energy of 0.45 J/cm^2 .

Table I shows the results of ρ_c and R_{sh} extracted from all the TLM measurements. In the RTA samples R_{sh} and ρ_c decrease as the formation temperature increases from 275 to 350 °C, except at 325 °C for which we do not have a physical explanation at present. In an overall sense, the RTA samples produce $\rho_c > 10^{-4}$ Ω.cm^2.

In general R_{sh} and ρ_c are lower in the LTA samples. The best ρ_c value is 2.84×10^{-7} Ω.cm^2 obtained for the TLM sample annealed at 0.45 J/cm^2, while $\rho_c = 1.33\times10^{-6}$ Ω.cm^2 produced by 0.35 J/cm^2 is also a significant result. These ρ_c values are 2-3 orders of magnitude lower than the equivalent RTA cases. It should be stressed again that the only process variable in this experimental work was the germanide formation anneal. It is interesting to see that increasing the LTA energy density to 0.55 J/cm^2 results in higher ρ_c. This could be attributed to the degradation of the interface quality.

Based on previous work we estimate the active doping concentration on the order of $3-6\times10^{19}$ cm^{-3}, depending on amount of P snowploughed by the growing germanide layer, on how much Ge is consumed, and on how much the germanide formation anneal boosts or detracts from the initial activation level.

Table I: R_{sh} and ρ_c values for germanide contacts formed by RTA and LTA.

Contact formation	R_{sh}(Ω/sq)	ρ_c (Ω.cm^2)
275 °C	196.1	6.31×10^{-4}
300 °C	186.0	1.61×10^{-4}
325 °C	216.3	9.57×10^{-4}
350 °C	169.0	1.35×10^{-4}
0.35 J/cm^2	163.6	1.38×10^{-6}
0.45 J/cm^2	147.9	2.84×10^{-7}
0.55 J/cm^2	192.0	8.34×10^{-4}

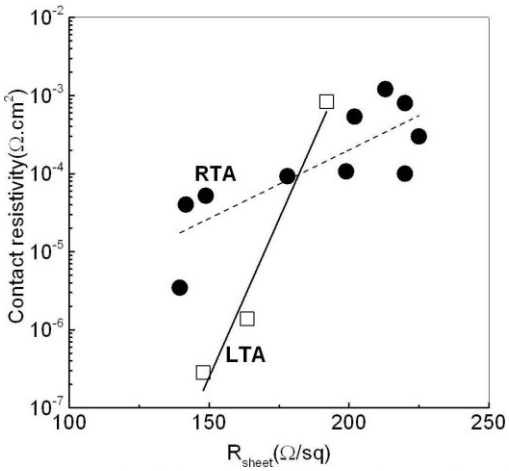

Fig. 10: ρ_c versus R_{sh} for all the samples in this work, as well as those from our previous NiGe on n-type Ge work using RTA [ref. 3]. For a *fixed* R_{sh} LTA can produce better ρ_c, if the correct energy density condition is selected.

It is well-known that ρ_c is a strong function of active doping in the substrate below the contact, thus any boost in dopant activation will yield a similar improvement in ρ_c. One might argue in this case for the 0.35 and 0.45 J/cm^2 LTA cases that the LTA is merely improving the P activation which is generating these ρ_c results. Indeed if one looks at Table I, it does seem that the R_{sh} values indicate LTA is a benefit for P activation. However if ρ_c versus R_{sh} is plotted, as in Fig. 10, one can immediately see that for a *fixed* R_{sh} LTA can still produce better ρ_c, if the correct energy density condition is selected. Note in Fig. 10, data points from our previous experiments on germanide formation by RTA are included for completeness [2]. Based on the divergent trend-lines it is argued here that LTA benefits ρ_c not only by boosting dopant activation, but by also improving the quality of the germanide-Ge interface. The latter could be responsible for reduced FLP, as reported by Lim et al. [11].

In the final part of this work, thermal stability of the germanide layers is explored. The ultra-short time and highly-localized energy densities of LTA processing may form highly non-equilibrium metastable conditions in the semiconductor materials and substrates. If this is the case thermal budget in the processes that come after the LTA process step, may cause any metastable condition revert back to a more equilibrium state. In order to evaluate germanide thermal stability one sample prepared at 300 °C RTA and one sample prepared by 0.45 J/cm^2 LTA were subjected to "post-processing" RTA treatments from 100 - 500 °C. The anneal times were 30 s each. Only one sample was post-processed for both RTA and

LTA so one should consider the post-processing thermal-budget in this study as cumulative. The inset of Fig 11 shows the TLM measurements of the LTA sample after post-processing. The slope and intercept of the fitted lines change after each RTA treatment, indicating that R_{sh} and ρ_c are deteriorated. Extracted ρ_c results are shown in Fig. 11.

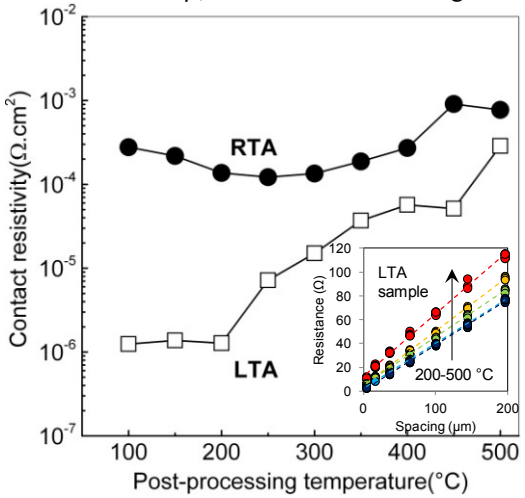

Fig. 11: ρ_c versus post-processing RTA treatments. Only one sample was post-processed for RTA and for LTA so one should consider the post-processing thermal-budget as cumulative. The inset shows resistance versus contact spacing after post-processing treatments. The anneal times were 30 s.

In the LTA sample ρ_c increases gradually, and at 250 °C there is a significant increase in resistivity. By 500 °C the ρ_c value is similar to the RTA cases. In the RTA sample ρ_c shows a slight decrease at 150 °C and then follows an increasing trend. Both samples were inspected by SEM (data not shown), and it was observed at the end of this post-processing anneal sequence that the germanide had agglomerated. It is well known that germanide layers annealed at 500 °C become agglomerated [14, 15].

There are various existing methods to alter thermal stability of silicide or germanide layers. One recent report highlighted the benefit of co-sputtering Ni and Pt prior to alloy formation [20]. In that work the addition of Pt improved the thermal stability of R_{sh} in the germanide layers

IV. Conclusions

The quality of germanide contacts formed by state-of-the-art LTA was investigated and compared systematically with RTA. LTA resulted in smoother layers of germanide, mainly NiGe and $NiGe_2$ with some epitaxial relation with the underlying Ge. The germanide-substrate interface was incredibly sharp without any detectable interfacial region or transition zone in HRTEM. Simulations indicated that the LTA melts a surface Ge layer, causing a liquid-solid reaction with the overlying Ni. The best contact resistivity obtained in this study was 2.84×10^{-7} $\Omega.cm^2$. Furthermore, the thermal stability of contacts formed by RTA and LTA was compared. Although LTA seems to be promising, it is imperative to explore solutions to improve thermal stability of contacts created by this approach.

References

[1] A. Dimoulas, P. Tsipas, A. Sotiropoulos, and E. K. Evangelou, "Fermi-level pinning and charge neutrality level in germanium," *Applied Physics Letters*, vol. 89, p. 252110, 2006.

[2] M. Shayesteh, C. L. L. M. Daunt, D. O'Connell, V. Djara, M. White, B. Long, and R. Duffy, "NiGe Contacts and Junction Architectures for P and As Doped Germanium Devices,", *IEEE Transactions on Electron Devices,* vol. 58, pp. 3801-3807, 2011.

[3] A. M. Roy, J. Lin, and K. C. Saraswat, "The Effect of Fixed Charge in Tunnel-Barrier Contacts for Fermi-Level Depinning in Germanium," *IEEE Electron Device Letters*, vol. 33, pp. 761-763, 2012.

[4] Y. Tong, B. Liu, P. S. Y. Lim, and Y. –C. Yeo, "Selenium Segregation for Effective Schottky Barrier Height Reduction in NiGe/n-Ge Contacts," *IEEE Electron Device Letters*, vol. 33, pp. 773-775, 2012.

[5] J.-R. Wu, Y.-H. Wu, C.-Y. Hou, M.-L. Wu, C.-C. Lin, and L.-L. Chen, "Impact of fluorine treatment on Fermi level depinning for metal/germanium Schottky junctions," Applied Physics Letters, vol. 99, pp. 253504-3, 2011.

[6] K. Gallacher, P. Velha, D. J. Paul, I. MacLaren, M. Myronov, and D. R. Leadley, "Ohmic contacts to n-type germanium with low specific contact resistivity," *Applied Physics Letters*, vol. 100, pp. 022113-3, 2012.

[7] Z. –W. Zheng, T. –C. Ku, M. Liu, and A. Chin, "Ohmic contact on n-type Ge using Yb-germanide", Applied Physics Letters vol. 101, p. 223501, 2012.

[8] W. B. Chen, B. S. Shie, Albert Chin, K. C. Hsu, and C. C. Chi, "*Higher k metal-gate/high-k/Ge n-MOSFETs with <1 nm EOT using laser annealing,*" in IEDM Tech. Dig., 2010, pp. 420-423.

[9] V. Mazzocchi, C. Sabatier, M. Py, K. Huet, C. Boniface, J. P. Barnes, L. Hutin, V. Delayer, D. Morel, M. Vinet, C. Le Royer, J. Venturini, and K. Yckache, "Boron and Phosphorus dopant activation in Germanium using laser annealing with and without preamorphization implant," in *17th International Conference on Advanced Thermal Processing of Semiconductors, RTP '09*. 2009, pp. 1-5.

[10] A. Firrincieli, K. Martens, R. Rooyackers, B. Vincent, E. Rosseel, E. Simoen, J. Geypen, H. Bender, C. Claeys, and J. A. Kittl, "Study of ohmic contacts to n-type Ge: Snowplow and laser activation," *Applied Physics Letters*, vol. 99, pp. 242104-3, 2011.

[11] P. S. Y. Lim, D. Z. Chi, X. C. Wang, and Y. –C. Yeo "Fermi-level depinning at the metal-germanium interface by the formation of epitaxial nickel digermanide NiGe2 using pulsed laser anneal," *Applied Physics Letters*, vol. 101, 172103, 2012.

[12] C. C. Liao, A. Chin, N. C. Su, M.-F. Li, and S. J. Wang, "*Low Vt Gate-First Al/TaN/[Ir3Si-HfSi2-x]/HfLaON CMOS Using Simple Laser Annealing/Reflection*" 2008 Symposium on VLSI Technology Digest of Technical Papers pp. 190-191.

[13] W. Szyszko, F. Vega, and C. N. Afonso, "Shifting of the thermal properties of amorphous germanium films upon relaxation and crystallization," *Applied Physics A*, vol. 61, pp. 141-147, 1995/08/01 1995.

[14] K. Lee, S. Liew, S. Chua, D. Chi, H. Sun, and X. Pan, "Formation and Morphology Evolution of Nickel Germanides on Ge (100) Under Rapid Thermal Annealing," Mat. Res. Soc. Symp. Proc. Vol. 810 2004, p. 55.

[15] Q. Zhang, N. Wu, T. Osipowicz, L. K. Bera, and C. Zhu, "Formation and thermal stability of nickel germanide on germanium substrate," *Japanese Journal of Applied Physics Part 2 Letters*, vol. 44, 2005.

[16] M. K. Husain, X. V. Li, and C. H. de Groot, "High-Quality Schottky Contacts for Limiting Leakage Currents in Ge-Based Schottky Barrier MOSFETs," IEEE Transactions on Electron Devices, vol. 56, pp. 499-504, 2009.

[17] P. S. Y. Lim, D. Z. Chi, P. C. Lim, X. C. Wang, T. K. Chan, T. Osipowicz, and Y.-C. Yeo, "Formation of epitaxial metastable NiGe2 thin film on Ge(100) by pulsed excimer laser anneal," *Applied Physics Letters*, vol. 97, pp. 182104-3, 2010.

[18] X. Gao, J. Andersson, T. Kubart, T. Nyberg, U. Smith, J. Lu, L. Hultman, A. J. Kellock, Z. Zhang, C. Lavoie, and S.-L. Zhang, "Epitaxy of Ultrathin NiSi2 Films with Predetermined Thickness," *Electrochemical and Solid-State Letters*, vol. 14, pp. H268-H270, January 1, 2011 2011.

[19] F. A. Trumbore, "Solid Solubilities of Impurity Elements in Germanium and Silicon," *Bell System Tech. J*, vol. 39, p. 205, 1960.

[20] M. –H. Kang, H. –S Shin, J. –H. Yoo, G. –W. Lee, J. –W. Oh, P. Majhi, R. Jammy, and H. –D. Lee, "Thermally Robust Ni Germanide Technology Using Cosputtering of Ni and Pt for High-Performance Nanoscale Ge MOSFETs," *IEEE Transactions on Nanotechnology*, vol. 11, pp. 769-776, 2012.

Maryam Shayesteh is currently working toward a Ph.D. in impurity doping and low-resistive contacts for advanced Germanium device applications at the Tyndall National Institute, University College Cork, Ireland.

Karim Huet is responsible for process and applications development involving experimental and simulation activities on Laser Thermal Annealing at Excico, France.

Inès Toqué-Tresonne obtained the Dipl.-Ing degree in optoelectronics from Polytech Paris-Sud engineering school in 2011. She is currently working as Application Engineer on Laser Thermal Annealing projects at Excico, France.

Răzvan Negru is currently working as Application Scientist in Excico, France. He is responsible for laser annealing technology simulation for a wide range of applications.

Chris L. M. Daunt is currently working towards the Ph.D. degree at the Tyndall National Institute. His current research interests include High Speed III-V optoelectronics components, and photonic integrated circuits.

Niall Kelly is currently undertaking a MSc degree with the aim of optimising metal ontact resistances for high speed photonic devices at Tyndall National Institute, Cork Ireland.

Dan O'Connell has worked in the III-V laboratory at Tyndall National Institute since 1993 where as a Senior Process Engineer he is responsible for a wide range of thin-film deposition and patterning processes.

Vladimir Djara is working toward the Ph.D. degree on the Physics of n-channel III-V MOSFETs at the Tyndall National Institute, University College Cork, Ireland.

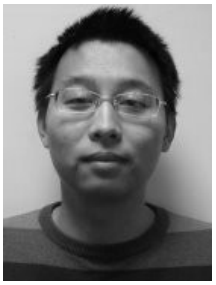

Ran Yu is currently working toward the Ph.D. degree, with particular emphasis on simulation, fabrication, and characterization of junctionless nanowire transistors, in the Tyndall National Institute, University College Cork, Cork, Ireland.

Patrick B. Carolan is an electron microscopist and joined the Tyndall National Institute in 2011, specialising in DB-SEM sample preparation and TEM imaging

Nikolay Petkov is leading a research area in advanced electron microscopy for analysis of semiconductor devices. His research interests are in-situ electron microscopy, materials processing and self-assembly.

Ray Duffy is at the Tyndall National Institute, where his activities include material science, process optimization, modeling, and device studies in Emerging Devices and Materials, for advanced semiconductor applications.